

# Analysis of the Performance of a Cloud Computing Processing Queue with Correlated Reneging of Tasks and Resubmission

1<sup>st</sup> Godlove Suila Kuaban  
*Institute of Theoretical and Applied Informatics*  
*Polish Academy of Sciences*  
Baltycka 5, 44–100 Gliwice, Poland  
gskuaban@iitis.pl

2<sup>nd</sup> Bhavneet Singh Soodan  
*Department of Mathematics*  
*Chandigarh University*  
Punjab, India, 140413  
bhavneet.e11868@cumail.in

3<sup>rd</sup> Rakesh Kumar  
*Department of Mathematics and Statistics*  
*Namibia University of Science and Technology*  
Namibia  
rkumar@nust.na

4<sup>th</sup> Piotr Czekalski  
*Department of Computer Graphics, Vision and Digital Systems,*  
*Silesian University of Technology*  
Akademicka 16, 44–100 Gliwice, Poland  
piotr.czekalski@polsl.pl

**Abstract**—The Quality of Service (QoS) experienced by the packets that constitute a cloud computing task does not only depend on the performance of the cloud computing network infrastructure at the data centre but also on the performance of the access networks and the internet core networks traversed by the packets before the task is fully submitted to the cloud computing or processing servers for execution or processing. Sometimes, some of the tasks that are submitted and are waiting in queues to be processed could be removed from the queues without being processed (task reneging or dropping). Removing tasks from the queue could result from the user's impatience, missing execution deadline, security reasons, or an active queue management strategy. The reneged or dropped tasks could be resubmitted depending on the reason for which it was dropped. The resubmission of tasks decreases QoS and increases the energy consumption overhead as more energy is required to transport the resubmitted tasks through the access, core, and data centre networks. In this paper, we propose a multiserver queueing model with correlated reneging and resubmission to analyse the performance of a cloud computing server.

**Index Terms**—Transient-state, steady-state, performance evaluations, cloud computing model, correlated reneging of tasks and resubmission

## I. INTRODUCTION

Cloud computing is an emerging paradigm which enables cloud service providers to offer computing services such as software, platforms, infrastructure, and other computing services to cloud computing users based on demand [1], [2]. It has significantly reduced the cost of setting-up and scaling-up information technology (IT) infrastructure and services. It has also emerged as the backbone of the modern economy, and have eliminated the need to develop and deploy the infrastructure and services from scratch. The time to set-up the IT infrastructure and services by enterprises, especially start-ups, have been significantly reduced. Therefore, it enables

cloud users to access various IT resources based on demand, and with low management overhead [3]. It also reduces security, storage, and the management cost incurred by the end-users, and provide development environment and tools for the application developers.

The cloud computing physical machine has been represented using queuing models in [1], [2], [4]–[8]. The authors in [4]–[6] used the M/M/c queuing model where the first M indicates that the inter-arrival times follow a Poisson arrival process while the second M indicates that the service times are exponentially distributed respectively, c is the number of virtual machines (VMs) assumed to be running in parallel, and the buffer size or the maximum queue size is infinite. However, the buffer size is not infinite as memory is a limited resource in computing systems. If there is no available space to store arriving tasks, the tasks that arrive when the buffer is full will be dropped, and this scenario should be considered when designing and planning cloud computing systems. The authors in [1], [2], [7], [8] used an M/M/c/K queuing model, where  $K = N + c$  and  $N$  is the buffer size. They derived the probability of task rejection or tail dropping when the buffer is full and incoming tasks are rejected continuously.

Not all the tasks stored in buffers in cloud computing servers are processed. After submitting a task, it could be possible for a user to cancel the task or renege for various reasons. A task could be dropped because its execution deadline has been exceeded, due to security reasons or as an active queue management strategy. The authors in [1], [2] proposed steady-state multiserver queueing models for the performance analysis of cloud computing servers with task reneging or dropping of tasks from the queues. The authors in [8] proposed queueing theory-based performance evaluation model for cloud computing servers with reneging

and resubmission of renege tasks.

The resubmission of tasks that have been dropped implies that the network must again allocate resources to transport the packets that constitute the dropped tasks from the users' devices through the access, core, and data centre networks and store the tasks again in the buffers in the cloud computing queues. Handling resubmitted tasks increases the traffic load and resource usage, decreasing the QoS and increasing the energy consumption in the access, core, and data centre networks. Hence, extra energy is required to receive, store, process, and transmit packets in network nodes. Increased energy consumption due to the handling of resubmitted tasks (in large scale data centres) increases the carbon emission (if energy is generated from fossil fuels) and also increase the operations cost for the cloud service provider.

The model proposed in the paper differ from the one proposed in [8] in that instead of considering that the renege times are exponential distributed, we assume that renege times are correlated. Correlated renege could be useful to model a scenario where the renege or dropping of a task from the queue, could trigger the renege or dropping of tasks that depend on it. In this paper, we propose a multi-server Markovian queuing model with correlated renege of tasks from queues in cloud computing servers and resubmission (or feedback) and use it to study the influence of correlated renege, arriving traffic of tasks, and resubmission probability on the performance parameters such as mean delay and the blocking probability in the transient state. We also present the steady-state performance analysis.

The rest of the paper is organised as follows: Section II contains a description of the cloud computing model with its corresponding queuing model with tasks renege or dropping, section III contains the proposed queuing model, section IV contains some numerical examples for performance evaluations, and section V contains the conclusion and future works.

## II. QUEUING MODEL DESCRIPTION

The tasks submitted by the users are transported over the internet to the cloud data centres, as shown in Figure 1. When tasks travel from the user devices, through the access networks and the internet core networks to the cloud computing servers where they are executed, they are delayed in queues formed within the various network devices. However, most of the performance evaluation studies of cloud computing services give the impression that the tasks are submitted directly to the cloud computing servers without any delay cost incurred as the task travels from the user device to the cloud servers. The delay budget can be given as

$$D = D_{link} + D_{access} + D_{core} + D_{cloud} \quad (1)$$

Where,  $D_{link}$  is the delay experienced by packets that constitute the tasks as they are propagated through the transmission medium (either wireless in the case of wireless access networks or wired in the case of some access and core networks). Also,  $D_{access}$ ,  $D_{core}$ , and  $D_{cloud}$  are the mean

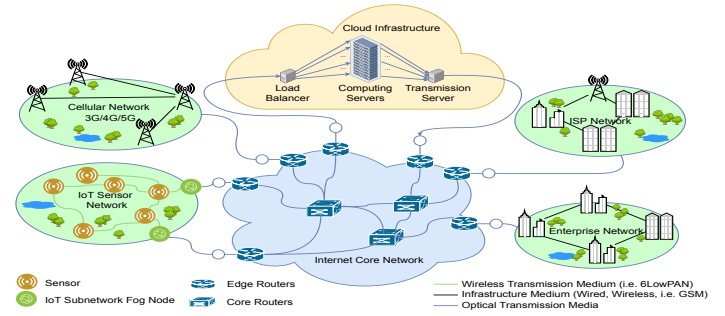


Fig. 1. Cloud computing model

delays experienced by the packets that constitute the task due to queuing and transmission in network devices at the access, core, and data centre networks respectively.

Queueing theory has been extensively applied to evaluate the performance of access and core networks (steady-state and transient state analysis of the delay and packet losses) [9], [10]. At the edge router, which acts as an interface between the access and the core network, smaller packets from the access networks (e.g., DSLs, Ethernet LANs, wireless LANs, IoT and 3G/4G/5G mobile networks) are aggregated into larger packets. The packets are converted into optical packets, transported through the optical core networks purely in the optical domain, and disaggregated at their destination. Packet aggregation increases bandwidth efficiency, ensure efficient use of network resources, and reduces energy consumption at the access, core, and data centre networks as demonstrated in [11]. Still, it introduces additional delays, which may be unacceptable for real-time applications (especially IoT real-time applications). It should be noted that with rapid advances in broadband networks and high-speed optical internet core networks, the delays experienced by the tasks as they travel from the access networks to the cloud servers have been significantly reduced. However, due to the variable times required to execute or process tasks in cloud computing servers, queues are inevitable, and the queuing delays may sometimes be significant.

When tasks arrive at the cloud computing data centre, they are scheduled to the respective physical machines by the load balancer. At the physical machine, the tasks are assigned to the respective VMs for execution. Each physical machine contains several VMs that processes or executes the tasks submitted by the users and return the results, which could be sent back to the users through the transmission servers. A simplified queuing model representation of a cloud computing data centre with task renege or dropping is shown in Figure 2.

It is assumed that the interarrival times of tasks at the task queue follows a Poisson process with parameter  $\lambda$  and that the service times are exponentially distributed with parameters  $\mu$ . The mean processing rate of tasks is:

$$\mu_n = \begin{cases} n\mu, & 0 \leq n < c \\ c\mu & c \leq n \leq N \end{cases} .$$

The maximum number of tasks at each queue is  $K = N + c$ ,

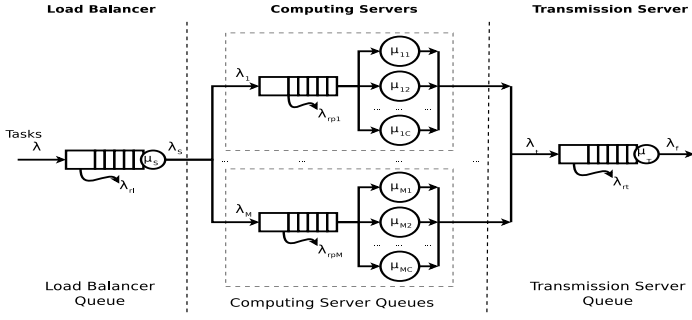


Fig. 2. Queuing model of a cloud computing data centre

where  $c$  is the number of VMs running in parallel and  $N$  is the size of the buffer in which the tasks are stored. Any task that is waiting in the queue can be dropped from the queue without being processed. When a task is dropped, other tasks that depends on it are likely to be dropped. A task that is dropped from the queue can be resubmitted with a probability,  $p_1$ , otherwise, it is not resubmitted with a probability of  $q_1 = 1 - p_1$ . Therefore, the reneing of the tasks can take place only at the transition marks  $t_0, t_1, t_2, \dots$  where  $\theta_r = t_r - t_{r-1}$ ,  $r = 1, 2, 3, \dots$ , are random variables with  $P[\theta_r \leq x] = 1 - \exp(-\xi x)$ ;  $\xi \geq 0$ ,  $r = 1, 2, 3, \dots$ . That is, the distribution of inter-transition marks is negative exponential with parameter  $\xi$ . The reneing at two consecutive transition marks is governed by the following transition probability matrix:

$$\begin{array}{c} \text{to } t_r \\ \begin{array}{c} 0 \\ 1 \end{array} \left\| \begin{array}{cc} 0 & 1 \\ p_{00} & p_{01} \\ p_{10} & p_{11} \end{array} \right\| \\ \text{from } t_{r-1} \end{array}$$

where  $p_{00} + p_{01} = 1$  and  $p_{10} + p_{11} = 1$ .

0 refers to no reneing and 1 refers to the occurrence of reneing. Thus, the reneing at two consecutive transition marks is correlated.

### III. QUEUING MODELLING

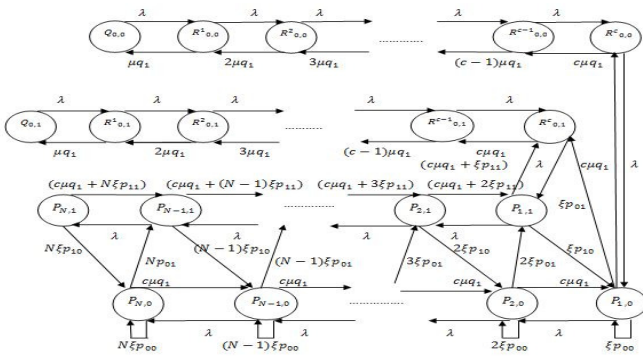


Fig. 3. The state transition diagram of the queuing model

Let  $X(t)$ ,  $t \geq 0$  be a random process that represent the number of tasks in the queue at time  $t$  and  $P\{X(t) = n\} = P_{n,r}(t)$  be the probability that there are  $n$  tasks in the queue at time  $t$ , where  $r = 1$  indicates that reneing has occurred at a previous transition mark otherwise, no reneing has occurred. Let us consider that the probability that at time  $t$ , there is no task in the buffer ( $n=0$ ) and that all the VMs are idle is  $Q_{0,r}(t)$ , and also consider that the probability that at time  $t$ , there is no task in the buffer and  $k$  ( $1 \leq k \leq c$ ) servers are active is  $R_{0,r}^k(t)$ . Also, suppose that the probability that at time  $t$ , the buffer is full ( $n=N$ ) is  $P_{N,r}(t)$ .

The difference-differential equations for the time-dependent state probabilities of the number of tasks in the queue obtained using the state transition diagram in Figure 3 are:

$$\frac{d}{dt} Q_{0,0}(t) = -\lambda Q_{0,0}(t) + \mu q_1 R_{0,0}^1(t) \quad (2)$$

$$\frac{d}{dt} R_{0,0}^1(t) = -(\lambda + \mu q_1) R_{0,0}^1(t) + 2\mu q_1 R_{0,0}^2(t) + \lambda Q_{0,0}(t) \quad (3)$$

$$\frac{d}{dt} R_{0,0}^k(t) = -(\lambda + k\mu q_1) R_{0,0}^k(t) + (k+1)\mu q_1 R_{0,0}^{k+1} + \lambda R_{0,0}^{k-1}(t), 1 < k < c \quad (4)$$

$$\frac{d}{dt} R_{0,0}^c(t) = -(\lambda + c\mu q_1) R_{0,0}^c(t) + c\mu q_1 P_{1,0} + \lambda R_{0,0}^{c-1}(t) \quad (5)$$

$$\frac{d}{dt} P_{1,0}(t) = -(\lambda + c\mu q_1 + \xi) P_{1,0}(t) + c\mu q_1 P_{2,0}(t) + \lambda R_{0,0}^c(t) + \xi [p_{00} P_{1,0}(t) + p_{10} P_{1,1}(t)] \quad (6)$$

$$\frac{d}{dt} P_{n,0}(t) = -(\lambda + c\mu q_1 + n\xi) P_{n,0}(t) + c\mu q_1 P_{n+1,0}(t) + \lambda P_{n-1,0}(t) + n\xi [p_{00} P_{n,0}(t) + p_{10} P_{n,1}(t)], 1 < n < N \quad (7)$$

$$\frac{d}{dt} P_{N,0}(t) = -(c\mu q_1 + N\xi) P_{N,0}(t) + \lambda P_{N-1,0}(t) + N\xi [p_{00} P_{N,0}(t) + p_{10} P_{N,1}(t)] \quad (8)$$

$$\frac{d}{dt} Q_{0,1}(t) = -\lambda Q_{0,1}(t) + \mu q_1 R_{0,1}^1(t) \quad (9)$$

$$\frac{d}{dt} R_{0,1}^1(t) = -(\lambda + \mu q_1) R_{0,1}^1(t) + 2\mu q_1 R_{0,1}^2(t) + \lambda Q_{0,1}(t) \quad (10)$$

$$\frac{d}{dt} R_{0,1}^k(t) = -(\lambda + k\mu q_1) R_{0,1}^k(t) + (k+1)\mu q_1 R_{0,1}^{k+1} + \lambda R_{0,1}^{k-1}(t), 1 < k < c \quad (11)$$

$$\frac{d}{dt} R_{0,1}^c(t) = -(\lambda + c\mu q_1) R_{0,1}^c(t) + c\mu q_1 P_{1,1} + \lambda R_{0,1}^{c-1}(t) + \xi [p_{11} P_{1,1}(t) + p_{01} P_{1,0}(t)] \quad (12)$$

$$\frac{d}{dt} P_{1,1}(t) = -(\lambda + c\mu q_1 + \xi) P_{1,1}(t) + c\mu q_1 P_{2,1}(t) + \lambda R_{0,1}^c(t) + 2\xi [p_{01} P_{2,0}(t) + p_{11} P_{2,1}(t)] \quad (13)$$

$$\frac{d}{dt} P_{n,1}(t) = -(\lambda + c\mu q_1 + n\xi) P_{n,1}(t) + c\mu q_1 P_{n+1,1}(t) + \lambda P_{n-1,1}(t) + (n+1)\xi [p_{01} P_{n+1,0}(t) + p_{11} P_{n+1,1}(t)], 1 < n < N \quad (14)$$

$$\frac{d}{dt}P_{N,1}(t) = -(c\mu q_1 + N\xi)P_{N,1}(t) + \lambda P_{N-1,1}(t) \quad (15)$$

In steady-state, the time-dependent variables of the queueing model in equations 2-15 becomes independent of time, that is:  $\lim_{t \rightarrow \infty} Q_{0,r}(t) = Q_{0,r}$ ,  $r = 0, 1$ ,  $\lim_{t \rightarrow \infty} R_{0,r}^k(t) = R_{0,r}^k$ ,  $k=1, 2, \dots, c$ ,  $r = 0, 1$  and  $\lim_{t \rightarrow \infty} P_{n,r}(t) = P_{n,r}$ ,  $n=0, 1, 2, \dots, N$  and  $r = 0, 1$ . Therefore, in steady-state, the differential equations above becomes simple linear equations (see equations 20-31 in the appendix-1). Detailed steady-state analysis of the presented model can be found in the appendix-1, but it will be easier to use standard solvers for systems of linear equations but for systems with fewer states, the presented methods can be used.

After obtaining the steady-state probabilities using the presented steady-state analysis, we can derive some steady-state performance evaluations parameters such as the mean number of tasks in the queue, the average rate at which tasks are being removed from the queue (reneging rate), the task loss probability resulting from task rejection (tail dropping of tasks from the queue), and the mean waiting time of tasks in the queue. The mean number of tasks in the queue is

$$L_q = \sum_{n=1}^N nP_{n,0} + \sum_{n=1}^N nP_{n,1} \quad (16)$$

Suppose that the tasks arrive in the queue when the buffer in which tasks are stored is full and will be rejected with a probability  $P_{N,r}$  (the probability for the state  $n = N$ , which can be obtained from the steady-state analysis), and that the instantaneous rejection rate of tasks from the queue is  $\lambda_r = \lambda(P_{N,0} + P_{N,1})$ . Also, suppose that any of the  $n$  tasks in the queue could be removed or could renege, then the average reneging rate is

$$R = \sum_{n=1}^N n\xi P_{n,0} + \sum_{n=1}^N n\xi P_{n,1} \quad (17)$$

The probability of losing tasks due to rejection of tasks when the buffer is full and due to the removal of tasks from the queue (reneging of users or task dropping) is [1], [2], [12]

$$p_l = \frac{\lambda_r + R}{\lambda} \quad (18)$$

We obtain the expected waiting time of tasks in the queue using Little's law, which is well known in queueing theory. The steady-state waiting time of tasks in the queue is

$$W_q = \frac{L_q}{\lambda(1 - P_{n,0} - P_{n,1})} \quad (19)$$

Therefore, the design parameters such as the buffer size  $N$ , the processing speed of the virtual machine  $s\mu$  (where  $s$  is the mean size of tasks and  $\mu$  is mean rate at which tasks are processed), and the number of virtual machines  $c$  should be chosen such that for a given traffic rate  $\lambda$ , the probability of losing tasks and the waiting time of task in the queue should be acceptable.

In the transient-state, it is difficult to analytically solve the set of differential equations in section 3 (equations

(2)-(15)) above. Therefore, we use a numerical method (Runge-Kutta method of fourth order) to obtain the transient solution of the model. The "ode45" function of the MATLAB software is used to solve equations (2)-(15) to obtain the transient performance results presented in the next section. The probability that at time  $t$ , the buffer is full ( $n=N$ ),  $P_{N,r}(t)$ , can be obtained by solving equations (2)-(15) numerically. The average waiting queue size and the average waiting time in transient state are given by

$$L_q(t) = \sum_{n=1}^N n[P_{n,0}(t) + P_{n,1}(t)]$$

$$W_q(t) = \frac{L_q(t)}{c\mu(1 - Q_{0,0}(t) - Q_{0,1}(t) - \sum_{k=1}^c (R_{0,0}^k(t) + R_{0,1}^k(t)))}$$

#### IV. NUMERICAL EXAMPLES

For all the graphs plotted, we take the initial condition as  $P_{1,0}(0) = 1$  (i.e. there is one task in the queue at time  $t = 0$ ),  $p_{00} = 0.8$ ,  $p_{01} = 0.2$ ,  $p_{10} = 0.7$  and  $p_{11} = 0.3$  (the probabilities  $p_{00}$ ,  $p_{01}$ ,  $p_{10}$  and  $p_{11}$  are chosen such that  $p_{00} + p_{01} = 1$  and  $p_{10} + p_{11} = 1$  as seen in section II).

Figure 4 shows the variation of the average delay experienced by tasks waiting in processing server queue with time and a comparison between the multi-server Markovian queueing model with feedback and correlated reneging, multi-server Markovian queueing model with correlated reneging and multi-server Markovian queueing model with feedback and reneging cases. It is observed that in the transient state, the average delay first increases and then attains the steady state after some time. For the queueing model with feedback and correlated reneging, the average delay is higher than the queueing model with correlated reneging, which shows the effect of feedback (resubmission of tasks), that is, more tasks are re-joining the queue, and hence, the tasks wait longer in the queue. Also, the average delay for the queueing model with feedback and correlated reneging is higher than the queueing model with feedback and simple reneging; however, it depends on the correlation between the dropping instants. If the reneging time instants have a high correlation, the dropping of tasks at one instant may result in the dropping of tasks that depend on it in future instants, and the queue size will reduce, leading to lower delays. The influence of correlation reneging is illustrated in figure 8 which shows the influence of transition marks on the average delay. A similar behaviour can be observed for the probability of task blocking as shown in figure 5.

Figures 6 and 7 show the influence of the average arrival rate of tasks on the average delay and the probability of task blocking, respectively. It can be observed that on increasing the value of the mean arrival rate, both the average delay and the probability of task blocking increase.

Figure 8 shows the influence of the rate of transition marks on the average delay. It can be seen that an increase in the rate of transition marks creates a decrease in the average delay. The higher the transition marks, the more instances where the reneging could occur and hence, decrease in the queue size and delay.

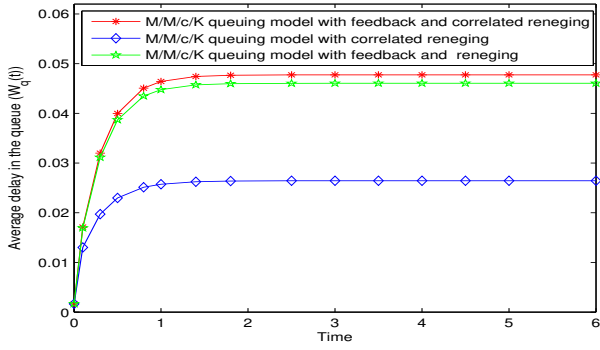


Fig. 4. Average delay in the queue vs. Time.  $\lambda = 580, \mu = 60, c = 10, q_1 = 0.9, \xi = 0.3, K = 50$

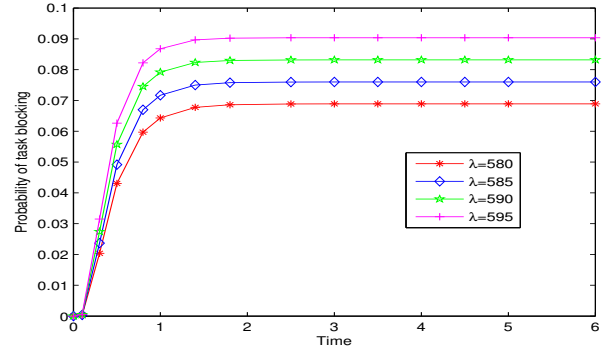


Fig. 7. Effect of average arrival rate on probability of task blocking.  $\mu = 60, c = 10, q_1 = 0.9, \xi = 0.3, K = 50$

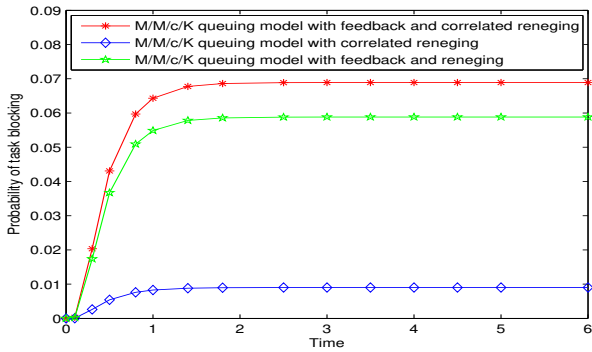


Fig. 5. Probability of task blocking vs. Time.  $\lambda = 580, \mu = 60, c = 10, q_1 = 0.9, \xi = 0.3, K = 50$

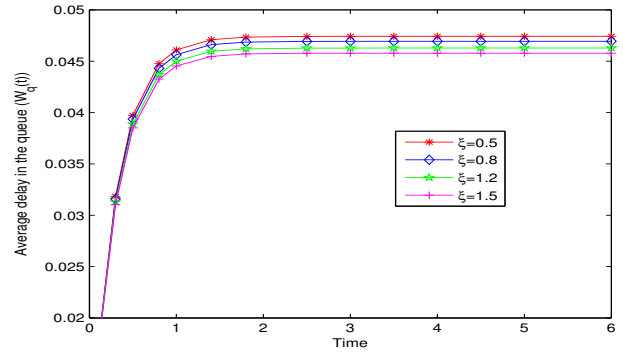


Fig. 8. Effect of rate of transition mark on average delay in the queue.  $\lambda = 580, \mu = 60, c = 10, q_1 = 0.9, K = 50$

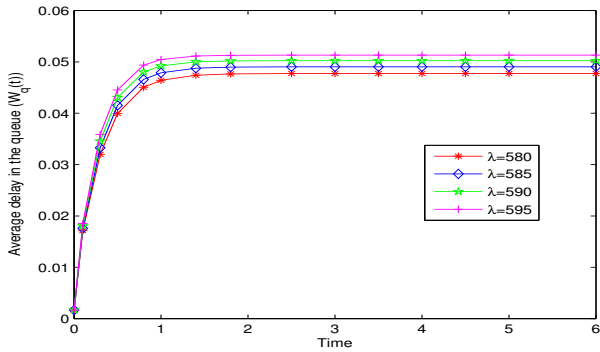


Fig. 6. Effect of average arrival rate on average delay in the queue.  $\mu = 60, c = 10, q_1 = 0.9, \xi = 0.3, K = 50$

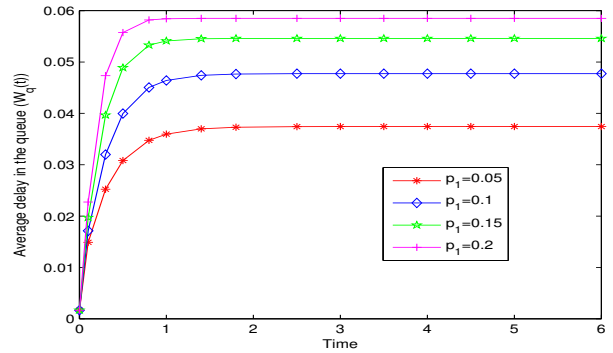


Fig. 9. Effect of probability of feedback on average delay in the queue.  $\lambda = 580, \mu = 60, c = 10, \xi = 0.3, K = 50$

Figure 9 illustrates the effect of the probability of feedback (resubmission) on average delay in the queue. It can be seen that with an increase in the probability of feedback, the average delay increases, which is quite obvious as resubmissions result in larger queue sizes and hence, increased delay.

## V. CONCLUSIONS

We have proposed a multiserver Markovian queuing model for the analysis of the performance of a cloud computing processing queue with correlated reneing or dropping of tasks from the queue. With the use of numerical examples, we demonstrated the influence of correlated reneing of tasks, the arriving traffic of tasks, and the probabilities of resubmission of tasks on the mean delay and the blocking probability in the

transient state. We also presented the steady-state performance analysis. Increasing the mean rate at which the tasks are submitted increases the mean delay and the probability of task blocking. Increasing the probability of task resubmission increases the delay and the blocking probability. Without resubmission, the delay and the probability of task blocking are smaller than the case with resubmission. The resubmission of tasks decreases QoS (i.e., increases delay, packet losses, and processing overhead). It also increases the energy consumption overhead as more energy is needed to transport the resubmitted tasks through the access, core, and data centre networks.

Even though Markovian queueing models have been used to evaluate the performance of cloud computing queues, they are limited by the assumption that the interarrival times of tasks into the queues follows a Poisson process and that the processing times are exponentially distributed. In reality, the tasks interarrival times and the processing times do not fully satisfy these assumptions but could be used to simplify the analysis. Attempts to perform steady-state and transient-state analysis of QoS in cloud computing using queueing models with general arrival times and general service times of tasks into the queues was discuss in [13], [14]. As a continuation of this work, diffusion approximation [15] to evaluate cloud computing queueing models with task reneging and resubmission using real traffic and realistic processing time can be used.

### Appendix-1

In steady-state, the difference equations describing the dynamic evolution of the queue reduces to:

$$0 = -\lambda R_{0,0}^1 + 2\mu q_1 R_{0,0}^2 \quad (20)$$

$$0 = -(\lambda + k\mu q_1)R_{0,0}^k + (k+1)\mu q_1 R_{0,0}^{k+1} + \lambda R_{0,0}^{k-1}, 1 \leq k < c \quad (21)$$

$$0 = -(\lambda + c\mu q_1)R_{0,0}^c + c\mu q_1 P_{1,0} + \lambda R_{0,0}^{c-1} \quad (22)$$

$$0 = -(\lambda + c\mu q_1 + \xi)P_{1,0} + c\mu q_1 P_{2,0} + \lambda R_{0,0}^c + \xi[p_{00}P_{1,0} + p_{10}P_{1,1}] \quad (23)$$

$$0 = -(\lambda + c\mu q_1 + n\xi)P_{n,0} + c\mu q_1 P_{n+1,0} + \lambda P_{n-1,0} + n\xi[p_{00}P_{n,0} + p_{10}P_{n,1}], 1 \leq n < N \quad (24)$$

$$0 = -(c\mu q_1 + N\xi)P_{N,0} + \lambda P_{N-1,0} + N\xi[p_{00}P_{N,0} + p_{10}P_{N,1}] \quad (25)$$

$$0 = -\lambda R_{0,1}^1 + 2\mu q_1 R_{0,1}^2 \quad (26)$$

$$0 = -(\lambda + k\mu q_1)R_{0,1}^k + (k+1)\mu q_1 R_{0,1}^{k+1} + \lambda R_{0,1}^{k-1}, 1 \leq k < c \quad (27)$$

$$0 = -(\lambda + c\mu q_1)R_{0,1}^c + c\mu q_1 P_{1,1} + \lambda R_{0,1}^{c-1} + \xi[p_{11}P_{1,1} + p_{01}P_{1,0}] \quad (28)$$

$$0 = -(\lambda + c\mu q_1 + \xi)P_{1,1} + c\mu q_1 P_{2,1} + \lambda R_{0,1}^c + 2\xi[p_{01}P_{2,0} + p_{11}P_{2,1}] \quad (29)$$

$$0 = -(\lambda + c\mu q_1 + n\xi)P_{n,1} + c\mu q_1 P_{n+1,1} + \lambda P_{n-1,1} + (n+1)\xi[p_{01}P_{n+1,0} + p_{11}P_{n+1,1}(t)], 1 \leq n < N \quad (30)$$

$$0 = -(c\mu q_1 + N\xi)P_{N,1} + \lambda P_{N-1,1} \quad (31)$$

Thus, the steady-state equations for (20)-(31) can be expressed in matrix-form as

$$\mathbf{P}\mathbf{Q} = \mathbf{0}. \quad (32)$$

$$\mathbf{Q} = \begin{pmatrix} -\lambda & \mathbf{A}_{12} & 0 & \mathbf{A}_{14} & 0 & \mathbf{A}_{16} & 0 & \mathbf{A}_{18} \\ \mathbf{A}_{21} & \mathbf{A}_{22} & \mathbf{A}_{23} & \mathbf{A}_{24} & \mathbf{A}_{25} & \mathbf{A}_{26} & \mathbf{A}_{27} & \mathbf{A}_{28} \\ 0 & \mathbf{A}_{32} & -(\lambda + c\mu q_1 + \xi + \xi p_{00}) & \mathbf{A}_{34} & 0 & \mathbf{A}_{36} & 0 & \mathbf{A}_{38} \\ \mathbf{A}_{41} & \mathbf{A}_{42} & \mathbf{A}_{43} & \mathbf{A}_{44} & \mathbf{A}_{45} & \mathbf{A}_{46} & \mathbf{A}_{47} & \mathbf{A}_{48} \\ 0 & \mathbf{A}_{52} & 0 & \mathbf{A}_{54} & -\lambda & \mathbf{A}_{56} & 0 & \mathbf{A}_{58} \\ \mathbf{A}_{61} & \mathbf{A}_{62} & \mathbf{A}_{63} & \mathbf{A}_{64} & \mathbf{A}_{65} & \mathbf{A}_{66} & \mathbf{A}_{67} & \mathbf{A}_{68} \\ 0 & \mathbf{A}_{72} & \xi p_{10} & \mathbf{A}_{74} & 0 & \mathbf{A}_{76} & -(\lambda + c\mu q_1 + \xi) & \mathbf{A}_{78} \\ \mathbf{A}_{81} & \mathbf{A}_{82} & \mathbf{A}_{83} & \mathbf{A}_{84} & \mathbf{A}_{85} & \mathbf{A}_{86} & \mathbf{A}_{87} & \mathbf{A}_{88} \end{pmatrix}$$

is a  $(2N + 2c) \times (2N + 2c)$  square matrix. Below are the each entry of the matrix Q:

$$\begin{aligned} \mathbf{A}_{12} &= (\lambda \ 0 \ \dots \ 0)_{1 \times c-1}, \mathbf{A}_{14} = (0 \ 0 \ \dots \ 0)_{1 \times N-1}, \\ \mathbf{A}_{21} &= \begin{pmatrix} 0 \\ \vdots \\ 0 \end{pmatrix}_{c-1 \times 1}, \mathbf{A}_{23} = \begin{pmatrix} 0 \\ \vdots \\ 0 \end{pmatrix}_{c-1 \times 1}, \\ \mathbf{A}_{16} &= (0 \ 0 \ \dots \ 0)_{1 \times c-1}, \mathbf{A}_{18} = (0 \ 0 \ \dots \ 0)_{1 \times N-1}, \\ \mathbf{A}_{22} &= \begin{pmatrix} -(\lambda + 2\mu q_1) & \lambda & \dots & 0 & 0 & 0 \\ 3\mu q_1 & -(\lambda + 3\mu q_1) & \dots & 0 & 0 & 0 \\ 0 & 4\mu q_1 & \dots & 0 & 0 & 0 \\ \vdots & \vdots & \ddots & \vdots & \vdots & \vdots \\ 0 & 0 & \dots & -(\lambda + (c-1)\mu q_1) & \lambda & 0 \\ 0 & 0 & \dots & c\mu q_1 & -(\lambda + c\mu q_1) & 0 \end{pmatrix}_{c-1 \times c-1}, \\ \mathbf{A}_{26} &= \begin{pmatrix} 0 & 0 & \dots & 0 & 0 \\ 0 & 0 & \dots & 0 & 0 \\ \vdots & \vdots & \ddots & \vdots & \vdots \\ 0 & 0 & \dots & 0 & 0 \\ 0 & 0 & \dots & 0 & 0 \end{pmatrix}_{c-1 \times c-1}, \mathbf{A}_{25} = \begin{pmatrix} 0 \\ \vdots \\ 0 \end{pmatrix}_{c-1 \times 1}, \\ \mathbf{A}_{27} &= \begin{pmatrix} 0 \\ \vdots \\ 0 \end{pmatrix}_{c-1 \times 1}, \mathbf{A}_{28} = \begin{pmatrix} 0 & 0 & \dots & 0 & 0 \\ 0 & 0 & \dots & 0 & 0 \\ \vdots & \vdots & \ddots & \vdots & \vdots \\ 0 & 0 & \dots & 0 & 0 \\ 0 & 0 & \dots & 0 & 0 \end{pmatrix}_{c-1 \times N-1}, \\ \mathbf{A}_{41} &= \begin{pmatrix} 0 \\ \vdots \\ 0 \end{pmatrix}_{N-1 \times 1}, \mathbf{A}_{24} = \begin{pmatrix} 0 & 0 & \dots & 0 & 0 \\ 0 & 0 & \dots & 0 & 0 \\ \vdots & \vdots & \ddots & \vdots & \vdots \\ 0 & 0 & \dots & 0 & 0 \\ 0 & 0 & \dots & 0 & 0 \end{pmatrix}_{c-1 \times N-1}, \\ \mathbf{A}_{32} &= (0 \ 0 \ \dots \ c\mu q_1)_{1 \times c-1}, \mathbf{A}_{34} = (\lambda \ 0 \ \dots \ 0)_{1 \times N-1}, \\ \mathbf{A}_{36} &= (0 \ 0 \ \dots \ \xi p_{01})_{1 \times c-1}, \\ \mathbf{A}_{38} &= (0 \ 0 \ \dots \ 0)_{1 \times N-1}, \mathbf{A}_{45} = \begin{pmatrix} 0 \\ \vdots \\ 0 \end{pmatrix}_{N-1 \times 1}, \\ \mathbf{A}_{83} &= \begin{pmatrix} 0 \\ \vdots \\ 0 \end{pmatrix}_{N-1 \times 1}, \mathbf{A}_{42} = \begin{pmatrix} 0 & 0 & \dots & 0 & 0 \\ 0 & 0 & \dots & 0 & 0 \\ \vdots & \vdots & \ddots & \vdots & \vdots \\ 0 & 0 & \dots & 0 & 0 \\ 0 & 0 & \dots & 0 & 0 \end{pmatrix}_{N-1 \times c-1}, \\ \mathbf{A}_{43} &= \begin{pmatrix} c\mu q_1 \\ \vdots \\ 0 \end{pmatrix}_{N-1 \times 1}, \mathbf{A}_{47} = \begin{pmatrix} 2\xi p_{01} \\ \vdots \\ 0 \end{pmatrix}_{N-1 \times 1}, \\ \mathbf{A}_{61} &= \begin{pmatrix} 0 \\ \vdots \\ 0 \end{pmatrix}_{c-1 \times 1}, \mathbf{A}_{46} = \begin{pmatrix} 0 & 0 & \dots & 0 & 0 \\ 0 & 0 & \dots & 0 & 0 \\ \vdots & \vdots & \ddots & \vdots & \vdots \\ 0 & 0 & \dots & 0 & 0 \\ 0 & 0 & \dots & 0 & 0 \end{pmatrix}_{N-1 \times c-1}, \\ \mathbf{A}_{63} &= \begin{pmatrix} 0 \\ \vdots \\ 0 \end{pmatrix}_{c-1 \times 1}, \mathbf{A}_{48} = \begin{pmatrix} 3\xi p_{01} & \dots & 0 & 0 & 0 \\ 0 & \dots & 0 & 0 & 0 \\ \vdots & \ddots & \vdots & \vdots & \vdots \\ 0 & \dots & 0 & 0 & 0 \\ 0 & \dots & N\xi p_{01} & 0 & 0 \end{pmatrix}_{N-1 \times N-1}, \end{aligned}$$

$$\begin{aligned}
\mathbf{A}_{52} &= (0 \ 0 \ \dots \ 0)_{1 \times c-1}, \\
\mathbf{A}_{54} &= (0 \ 0 \ \dots \ 0)_{1 \times N-1}, \\
\mathbf{A}_{56} &= (\lambda \ 0 \ \dots \ 0)_{1 \times c-1}, \mathbf{A}_{58} = (0 \ 0 \ \dots \ 0)_{1 \times N-1}, \\
\mathbf{A}_{62} &= \begin{pmatrix} 0 & 0 & \dots & 0 & 0 \\ 0 & 0 & \dots & 0 & 0 \\ 0 & 0 & \dots & 0 & 0 \\ \vdots & \vdots & \ddots & \vdots & \vdots \\ 0 & 0 & \dots & 0 & 0 \\ 0 & 0 & \dots & 0 & 0 \\ 0 & 0 & \dots & 0 & 0 \\ 0 & 0 & \dots & 0 & 0 \end{pmatrix}_{c-1 \times c-1}, \\
\mathbf{A}_{64} &= \begin{pmatrix} 0 & 0 & \dots & 0 & 0 \\ 0 & 0 & \dots & 0 & 0 \\ 0 & 0 & \dots & 0 & 0 \\ \vdots & \vdots & \ddots & \vdots & \vdots \\ 0 & 0 & \dots & 0 & 0 \\ 0 & 0 & \dots & 0 & 0 \\ 0 & 0 & \dots & 0 & 0 \\ 0 & 0 & \dots & 0 & 0 \end{pmatrix}_{c-1 \times N-1}, \\
\mathbf{A}_{66} &= \begin{pmatrix} -(\lambda+2\mu q_1) & \lambda & \dots & 0 \\ 3\mu & -(\lambda+3\mu q_1) & \dots & 0 \\ 0 & 4\mu & \dots & 0 \\ \vdots & \vdots & \ddots & \vdots \\ 0 & 0 & \dots & 0 \\ 0 & 0 & \dots & -(\lambda+c\mu q_1) \end{pmatrix}_{c-1 \times c-1}, \\
\mathbf{A}_{68} &= \begin{pmatrix} 0 & 0 & \dots & 0 & 0 \\ 0 & 0 & \dots & 0 & 0 \\ 0 & 0 & \dots & 0 & 0 \\ \vdots & \vdots & \ddots & \vdots & \vdots \\ 0 & 0 & \dots & 0 & 0 \\ 0 & 0 & \dots & 0 & 0 \\ 0 & 0 & \dots & 0 & 0 \\ 0 & 0 & \dots & 0 & 0 \end{pmatrix}_{c-1 \times N-1}, \mathbf{A}_{65} = \begin{pmatrix} 2\mu q_1 \\ 0 \\ \vdots \\ 0 \\ 0 \end{pmatrix}_{c-1 \times 1}, \\
\mathbf{A}_{67} &= \begin{pmatrix} 0 \\ 0 \\ \vdots \\ 0 \\ \lambda \end{pmatrix}_{c-1 \times 1}, \mathbf{A}_{81} = \begin{pmatrix} 0 \\ 0 \\ \vdots \\ 0 \\ 0 \end{pmatrix}_{N-1 \times 1}, \\
\mathbf{A}_{72} &= (0 \ 0 \ \dots \ 0)_{1 \times c-1}, \mathbf{A}_{74} = (0 \ 0 \ \dots \ 0)_{1 \times N-1}, \\
\mathbf{A}_{76} &= (0 \ \dots \ (c\mu q_1 + \xi p_{11}))_{1 \times c-1}, \mathbf{A}_{78} = (\lambda \ 0 \ \dots \ 0)_{1 \times N-1}, \\
\mathbf{A}_{86} &= \begin{pmatrix} 0 & 0 & \dots & 0 & 0 \\ 0 & 0 & \dots & 0 & 0 \\ 0 & 0 & \dots & 0 & 0 \\ \vdots & \vdots & \ddots & \vdots & \vdots \\ 0 & 0 & \dots & 0 & 0 \\ 0 & 0 & \dots & 0 & 0 \\ 0 & 0 & \dots & 0 & 0 \\ 0 & 0 & \dots & 0 & 0 \end{pmatrix}_{N-1 \times c-1}, \\
\mathbf{A}_{82} &= \begin{pmatrix} 0 & 0 & \dots & 0 & 0 \\ 0 & 0 & \dots & 0 & 0 \\ 0 & 0 & \dots & 0 & 0 \\ \vdots & \vdots & \ddots & \vdots & \vdots \\ 0 & 0 & \dots & 0 & 0 \\ 0 & 0 & \dots & 0 & 0 \\ 0 & 0 & \dots & 0 & 0 \\ 0 & 0 & \dots & 0 & 0 \end{pmatrix}_{N-1 \times c-1}, \\
\mathbf{A}_{85} &= \begin{pmatrix} 0 \\ 0 \\ \vdots \\ 0 \\ 0 \end{pmatrix}_{N-1 \times 1}, \mathbf{A}_{87} = \begin{pmatrix} c\mu q_1 + 2\xi p_{11} \\ 0 \\ \vdots \\ 0 \\ 0 \end{pmatrix}_{N-1 \times 1}, \\
\mathbf{A}_{44} &= \begin{pmatrix} -(\lambda+c\mu q_1+2\xi+2\xi p_{00}) & \dots & 0 & 0 & 0 \\ c\mu q_1 & \dots & 0 & 0 & 0 \\ \vdots & \ddots & \vdots & \vdots & \vdots \\ 0 & \dots & 0 & 0 & 0 \\ 0 & \dots & -(\lambda+c\mu q_1+2\xi+2\xi p_{00}) & 0 & 0 \end{pmatrix}_{N-1 \times N-1}, \\
\mathbf{A}_{84} &= \begin{pmatrix} 2\xi p_{10} & 0 & \dots & 0 & 0 \\ 0 & 3\xi p_{10} & \dots & 0 & 0 \\ 0 & 0 & \dots & 0 & 0 \\ \vdots & \vdots & \ddots & \vdots & \vdots \\ 0 & 0 & \dots & 0 & 0 \\ 0 & 0 & \dots & (N-1)\xi p_{10} & 0 \\ 0 & 0 & \dots & 0 & N\xi p_{10} \end{pmatrix}_{N-1 \times N-1}, \\
\mathbf{A}_{88} &= \begin{pmatrix} -(\lambda+c\mu q_1+2\xi) & \lambda & \dots & 0 \\ (c\mu q_1+3\xi p_{11}) & -(\lambda+c\mu q_1+3\xi) & \dots & 0 \\ 0 & (c\mu q_1+4\xi p_{11}) & \dots & 0 \\ \vdots & \vdots & \ddots & \vdots \\ 0 & 0 & \dots & 0 \\ 0 & 0 & \dots & -(\lambda+c\mu q_1+2\xi) \end{pmatrix}_{N-1 \times N-1}
\end{aligned}$$

Where,  $\mathbf{A}_{16}$ ,  $\mathbf{A}_{52}$  and  $\mathbf{A}_{72}$  are the row vectors of order  $c-1$  with all their entries as zeros.  $\mathbf{A}_{14}$ ,  $\mathbf{A}_{18}$ ,  $\mathbf{A}_{38}$ ,  $\mathbf{A}_{54}$ ,  $\mathbf{A}_{58}$ , and  $\mathbf{A}_{74}$  are also the row vectors of order  $N-1$  with all their entries as zeros.  $\mathbf{A}_{25}$ ,  $\mathbf{A}_{27}$ ,  $\mathbf{A}_{61}$  and  $\mathbf{A}_{63}$  are the column vectors of order  $c-1$  with all their entries as zeros.  $\mathbf{A}_{41}$ ,  $\mathbf{A}_{45}$ ,  $\mathbf{A}_{81}$ ,  $\mathbf{A}_{83}$  and  $\mathbf{A}_{85}$  are also column vectors of order  $N-1$  with all their

entries as zeros.  $\mathbf{A}_{26}$ ,  $\mathbf{A}_{28}$ ,  $\mathbf{A}_{24}$ ,  $\mathbf{A}_{42}$ ,  $\mathbf{A}_{46}$ ,  $\mathbf{A}_{62}$ ,  $\mathbf{A}_{64}$ ,  $\mathbf{A}_{68}$ ,  $\mathbf{A}_{82}$  and  $\mathbf{A}_{86}$  are square matrices with all their entries as zeros.

From the equation (32) it follows that

$$-\lambda R_{0,0}^1 + \mathbf{R}_0 \mathbf{A}_{21} = 0 \quad (33)$$

$$R_{0,0}^1 \mathbf{A}_{12} + \mathbf{R}_0 \mathbf{A}_{22} + P_{1,0} \mathbf{A}_{32} = 0 \quad (34)$$

$$\begin{aligned} \mathbf{R}_0 \mathbf{A}_{23} - (\lambda + c\mu q_1 + \xi + \xi p_{00}) P_{1,0} \\ + \mathbf{P}_0 \mathbf{A}_{43} + \xi p_{10} P_{1,1} = 0 \end{aligned} \quad (35)$$

$$P_{1,0} \mathbf{A}_{34} + \mathbf{P}_0 \mathbf{A}_{44} + \mathbf{P}_1 \mathbf{A}_{84} = 0 \quad (36)$$

$$-\lambda R_{0,1}^1 + \mathbf{R}_1 \mathbf{A}_{65} = 0 \quad (37)$$

$$\begin{aligned} P_{1,0} \mathbf{A}_{36} + R_{0,1}^1 \mathbf{A}_{56} + \mathbf{R}_1 \mathbf{A}_{66} \\ + P_{1,1} \mathbf{A}_{76} = 0 \end{aligned} \quad (38)$$

$$\mathbf{P}_0 \mathbf{A}_{47} + \mathbf{R}_1 \mathbf{A}_{67}$$

$$-P_{1,1}(\lambda + c\mu q_1 + \xi) + \mathbf{P}_1 \mathbf{A}_{87} = 0 \quad (39)$$

$$\mathbf{P}_0 \mathbf{A}_{48} + P_{1,1} \mathbf{A}_{78} + \mathbf{P}_1 \mathbf{A}_{88} = 0 \quad (40)$$

From equation (33), we get

$$R_{0,0}^1 = \frac{1}{\lambda} \mathbf{R}_0 \mathbf{A}_{21} \quad (41)$$

Substitute  $R_{0,0}^1$  from (41) to (34) we get

$$\mathbf{R}_0 = \frac{-\lambda P_{1,0} \mathbf{A}_{32}}{\mathbf{A}_{21} \mathbf{A}_{12} + \lambda \mathbf{A}_{22}} \quad (42)$$

Again putting  $\mathbf{R}_0$  from (42) to (33), on solving we get

$$R_{0,0}^1 = -\frac{P_{1,0} \mathbf{A}_{32} \mathbf{A}_{21}}{\mathbf{A}_{21} \mathbf{A}_{12} + \lambda \mathbf{A}_{22}} \quad (43)$$

(36), we get

$$\mathbf{P}_1 = -(\mathbf{P}_0 \mathbf{A}_{44} + P_{1,0} \mathbf{A}_{34}) \mathbf{A}_{84}^{-1} \quad (44)$$

Substituting the value of  $\mathbf{P}_1$  from (44) to (40), and solving we get

$$\mathbf{P}_0 = \frac{(P_{1,0} \mathbf{A}_{34} \mathbf{A}_{84}^{-1} \mathbf{A}_{88} - P_{1,1} \mathbf{A}_{78})}{(\mathbf{A}_{48} - \mathbf{A}_{44} \mathbf{A}_{84}^{-1} \mathbf{A}_{88})} \quad (45)$$

Putting the value of  $\mathbf{P}_0$  and  $\mathbf{R}_0$  from (45) and (42) respectively in (35), and solving

$$P_{1,1} = \frac{\left( \frac{\lambda \mathbf{A}_{32} \mathbf{A}_{23}}{\mathbf{A}_{21} \mathbf{A}_{12} + \lambda \mathbf{A}_{22}} + (\lambda + c\mu q_1 + \xi + \xi p_{00}) - \frac{\mathbf{A}_{34} \mathbf{A}_{84}^{-1} \mathbf{A}_{88} \mathbf{A}_{43}}{\mathbf{A}_{48} - \mathbf{A}_{44} \mathbf{A}_{84}^{-1} \mathbf{A}_{88}} \right) P_{1,0}}{\xi p_{10} - \left( \frac{\mathbf{A}_{78} \mathbf{A}_{43}}{\mathbf{A}_{48} - \mathbf{A}_{44} \mathbf{A}_{84}^{-1} \mathbf{A}_{88}} \right)} \quad (46)$$

$$\mathbf{P}_{1,1} = \mathbf{\Psi}_1 P_{1,0} \quad (47)$$

where,

$$\mathbf{\Psi}_1 = \frac{\left( \frac{\lambda \mathbf{A}_{32} \mathbf{A}_{23}}{\mathbf{A}_{21} \mathbf{A}_{12} + \lambda \mathbf{A}_{22}} + (\lambda + c\mu q_1 + \xi + \xi p_{00}) - \frac{\mathbf{A}_{34} \mathbf{A}_{84}^{-1} \mathbf{A}_{88} \mathbf{A}_{43}}{\mathbf{A}_{48} - \mathbf{A}_{44} \mathbf{A}_{84}^{-1} \mathbf{A}_{88}} \right)}{\xi p_{10} - \left( \frac{\mathbf{A}_{78} \mathbf{A}_{43}}{\mathbf{A}_{48} - \mathbf{A}_{44} \mathbf{A}_{84}^{-1} \mathbf{A}_{88}} \right)}$$

Substituting the value of  $\mathbf{P}_0$  from (47) to (45), and

solve we get

$$\mathbf{P}_0 = \frac{(\mathbf{A}_{34}\mathbf{A}_{84}^{-1}\mathbf{A}_{88} - \Psi_1\mathbf{A}_{78})P_{1,0}}{\mathbf{A}_{48} - \mathbf{A}_{44}\mathbf{A}_{84}^{-1}\mathbf{A}_{88}} \quad (48)$$

where,  $\Psi_2 = \frac{(\mathbf{A}_{34}\mathbf{A}_{84}^{-1}\mathbf{A}_{88} - \Psi_1\mathbf{A}_{78})}{\mathbf{A}_{48} - \mathbf{A}_{44}\mathbf{A}_{84}^{-1}\mathbf{A}_{88}}$

$$\mathbf{P}_0 = \Psi_2 P_{1,0} \quad (49)$$

From (37), we get

$$R_{0,1}^1 = \frac{\mathbf{R}_1 \mathbf{A}_{65}}{\lambda} \quad (50)$$

Putting value of  $R_{0,1}^1$  and  $P_{1,1}$  from (50) and (47) respectively in (38), On solving

$$\mathbf{R}_1 = \frac{-\lambda(\mathbf{A}_{36} + \Psi_1\mathbf{A}_{76})P_{1,0}}{\mathbf{A}_{65}\mathbf{A}_{56} + \lambda\mathbf{A}_{66}} \quad (51)$$

$$\mathbf{R}_1 = \lambda\Psi_3 P_{1,0} \quad (52)$$

where,  $\Psi_3 = -\frac{(\mathbf{A}_{36} + \Psi_1\mathbf{A}_{76})}{\mathbf{A}_{65}\mathbf{A}_{56} + \lambda\mathbf{A}_{66}}$   
 Putting the value of  $\mathbf{R}_1$  from (52) in (50). We get

$$R_{0,1}^1 = \Psi_3 \mathbf{A}_{65} P_{1,0} \quad (53)$$

Substituting the value of  $\mathbf{P}_0$  from (49) in (44). We get the value of  $\mathbf{P}_1$  as:

$$P_1 = -(\Psi_2\mathbf{A}_{44} + \mathbf{A}_{34})\mathbf{A}_{84}^{-1}P_{1,0} \quad (54)$$

We can obtain the value of  $Q_{0,0}$  and  $Q_{0,1}$  by substituting the value of  $R_{0,0}^1$  and  $R_{0,1}^1$  from (43) and (53) in (??) and (20) respectively.

$$Q_{0,0} = \frac{\mu q_1 \mathbf{A}_{32} \mathbf{A}_{21} P_{1,0}}{\lambda(\mathbf{A}_{21} \mathbf{A}_{12} + \lambda \mathbf{A}_{22})} \quad (55)$$

$$Q_{0,1} = \frac{\mu q_1 \Psi_3 \mathbf{A}_{65} P_{1,0}}{\lambda} \quad (56)$$

We can obtain the unknown constant  $P_{1,0}$  by using normalization equations:

$$\sum_{i=0}^1 Q_{0,i} + \sum_{k=1}^c \sum_{i=0}^1 R_{0,i}^k + \sum_{n=1}^N \sum_{i=0}^1 P_{n,i} = Q_{0,0} + R_{0,0}^1 + \mathbf{R}_0 \mathbf{e} + P_{1,0} + \mathbf{P}_0 \mathbf{e} + Q_{0,1} + R_{0,1}^1 + \mathbf{R}_1 \mathbf{e} + P_{1,1} + \mathbf{P}_1 \mathbf{e} = 1 \quad (57)$$

where  $\mathbf{e}$  is the unit column vector of dimension  $N$ .

Substituting the values of probabilities from equations (42), (43),(47),(49),(52),(53), (54),(55) and (56) in (57), we get the explicit expression for  $P_{1,0}$  as:

$$P_{1,0} = \frac{1}{[\Psi_4 + \Psi_5 + \Psi_6 \mathbf{e} + 1 + \Psi_2 \mathbf{e} + \frac{\mu q_1 \Psi_3 \mathbf{A}_{65}}{\lambda} + \Psi_3 \mathbf{A}_{65} + \lambda \Psi_3 \mathbf{e} + \Psi_1 - \Psi_7 \mathbf{e}]} \quad (58)$$

where,  $\Psi_4 = \frac{-\mu q_1 \mathbf{A}_{32} \mathbf{A}_{21}}{\lambda(\mathbf{A}_{21} \mathbf{A}_{12} + \lambda \mathbf{A}_{22})}$ ,  $\Psi_5 = -\frac{\mathbf{A}_{32} \mathbf{A}_{21}}{\mathbf{A}_{21} \mathbf{A}_{12} + \lambda \mathbf{A}_{22}}$ ,  $\Psi_6 = -\frac{\lambda \mathbf{A}_{32}}{\mathbf{A}_{21} \mathbf{A}_{12} + \lambda \mathbf{A}_{22}}$  and  $\Psi_7 = -(\Psi_2 \mathbf{A}_{44} + \mathbf{A}_{34})\mathbf{A}_{84}^{-1}$ . Thus, the rest of the steady-state probabilities of the model can be obtained explicitly using (42),(43),(47),(49),(52),(53), (54),(55) and (56) .

## REFERENCES

- [1] Y.-J. Chiang, Y.-C. Ouyang, and C.-H. Hsu, "Performance and cost-effectiveness analyses for cloud services based on rejected and impatient users," *IEEE Transactions on Services Computing*, vol. 9, no. 3, pp. 446–455, 2016.
- [2] Y.-J. Chiang and Y.-C. Ouyang, "Profit optimization in sla-aware cloud services with a finite capacity queuing model," *Mathematical Problems in Engineering*, pp. 1–11, 2014.
- [3] Y. Han, J. Chan, T. Alpcan, , and C. Leckie, "Using virtual machine allocation policies to defend against co-resident attacks in cloud computing," *IEEE Transactions on Dependable and Secure Computing*, vol. 14, no. 1, pp. 95–108, 2017.
- [4] L. Guo, T. Yan, S. Zhao, and C. Jiang, "Dynamic performance optimization for cloud computing using m/m/m queueing system," *Mathematical Problems in Engineering*, pp. 1–8, 2014.
- [5] Y. A. E. Mahjoub, J.-M. Fourneau, and H. Castel-Tale, "Analysis of energy consumption in cloud center with tasks migrations," in *Proceedings of the 2019 Computer Network Conference*, P. G. et al., Ed. kamień Śląski: Springer, 2019, pp. 301–315.
- [6] G. Huang, S. Wang, M. Zhang, Y. Li, Z. Qian, Y. Chen, and S. Zhang, "Auto scaling virtual machines for web applications with queueing theory," in *Proceedings of the The 2016 3rd International Conference on Systems and Informatics (ICSAI 2016)*. Shanghai: IEEE, 2016, pp. 433–438.
- [7] N. Neelima, B. Rao, G. Rao, and K.Chandan, "Performance analysis of web application deployment on cloud using m/m/s/k queueing model," *International Journal of Applied Engineering Research*, vol. 13, no. 11, pp. 9485–9492, 2018.
- [8] G. S. Kuaban, B. S. Soodan, R. Kumar, and P. Czekalski, "Performance evaluations of a cloud computing physical machine with task renegeing and task resubmission (feedback)," in *Proceedings of the International Conference on Computer Networks (CN2020)*, P. G. et al., Ed. Gdansk, Poland: Springer, 2020, pp. 185–198.
- [9] T. Czachórski, E. Gelenbe, G. S. Kuaban, and D. Marek, "Time-dependent performance of a multi-hop software defined network," *Applied Sciences*, vol. 11, no. 2469, pp. 1–21, 2021.
- [10] —, "Transient behaviour of a network router," in *Proceedings of the 43th International Conference on Telecommunications and Signal Processing (TSP)*. Milan, Italy: IEEE, 2020, pp. 246–252.
- [11] G. S. Kuaban, T. Atmaca, and T. C. and, "Performance analysis of packet aggregation mechanisms and their applications in access (e.g., iot, 4g/5g), core, and data centre networks," *Sensors*, vol. 21, no. 3898, pp. 1–33, 2021.
- [12] G. S. Kuaban, R. Kumar, and B. S. Soodan, "A multi-server queueing model with balking and correlated renegeing with application in health care management," *IEEE Access*, vol. 8, pp. 169 623–169 639, 2020.
- [13] T. Czachórski and K. Grochla, "Diffusion approximation models for cloud computations with task migrations," in *Proceedings of the 2019 IEEE International Conference on Fog Computing (ICFC)*. Milan, Italy: IEEE, 2019, pp. 27–30.
- [14] T. Czachórski, G. S. Kuaban, and T. Nycz, "Multichannel diffusion approximation models for the evaluation of multichannel communication networks," in *Distributed Computer and Communication Networks. DCCN 2019. Lecture Notes in Computer Science*, K. D. e. Vishnevskiy V., Samouylov K., Ed., vol. 11965. Moscow, Russia: Springer, 2019, pp. 43–57.
- [15] E. Gelenbe, "On approximate computer system models," *Journal of the ACM (JACM)*, vol. 22, no. 2, pp. 261–269, 1975.